

# High Resolution DF Architectures Using a Robust Symmetric Number System Encoding

*D.J. Wickersham, P.E. Pace, D. Styer, D.C. Jenn, R. Vitale and N.S. York*

Center for Joint Services Electronic Warfare  
Department of Electrical and Computer Engineering  
Naval Postgraduate School  
Monterey, CA 93943, USA  
pepace@nps.navy.mil

**Abstract:** A direction finding architecture that implements an innovative number system encoding of phase samples, the robust symmetric number system (RSNS), is described. The RSNS possesses Gray Code properties and provides significant advantages over conventional phase scanning methods and other symmetric number system encoding techniques. The design equations for a RSNS array are presented. Simulation results for a prototype RSNS array are shown, and its performance compared to previously published results for other number system encoded direction finding architectures.

## I. Introduction

Direction finding systems provide an emitter's bearing that can be used as a sorting parameter in the identification of radar and communication systems. The phase sampled linear interferometer is a common DF approach that uses the known spacing between two or more array elements to obtain time-of-arrival measurements [1]. The time-of-arrival measurements can be converted into phase differences that are then used to determine the angle of arrival (AOA).

This paper describes the development of a new type of phase-sampled DF array based on the robust symmetrical number system (RSNS) [2]. The RSNS DF antenna architecture uses the RSNS to decompose the analog spatial filtering operation into a number of parallel sub-operations or moduli that are of smaller complexity. One two-element interferometer is used for each sub-operation and only requires a precision in accordance with its modulus. A much higher spatial resolution is achieved after the spatial filtering results from the individual low-resolution arrays are recombined.

## II. RSNS Antenna Architecture

The RSNS DF array is a modular scheme in that the integer values within each modulus (phase sampling comparator states), when considered together, change one at a time between adjacent positions (a Gray code property). Although the dynamic range of the RSNS is somewhat less than that of the optimum SNS (OSNS) [3], the RSNS Gray code properties make it particularly attractive for error control. With RSNS encoding, the errors due to comparator thresholds not being crossed simultaneously are eliminated. As a result, the interpolation circuits can be removed, and only a small number of comparators are required.

Table 1 illustrates a RSNS and compares it to an OSNS for the two moduli case. The shaded cells (bins) are unique combinations of integers, that are mapped into spatial angles over the antenna's field of view (FOV). The entries also correspond to the number of comparators ON in each channel. The DF resolution is the FOV divided by the number of unique combinations (shaded cells). The number of unique combinations is also referred to as the dynamic range. From computer results the dynamic range,  $\hat{M}$ , for a two-channel system is conjectured to be [2]:

$$\hat{M} = 4m_1 + 2m_2 - 5, \text{ for moduli spaced 1 or 2 apart, and} \quad (1)$$

$$\hat{M} = 4m_1 + 2m_2 - 2, \text{ for moduli spaced 3 or more apart.} \quad (2)$$

The dynamic range of the OSNS is the product of the moduli. The dynamic range of the OSNS grows faster than the RSNS dynamic range, so for practical systems (which require dynamic ranges greater than 50), the OSNS can achieve larger values with smaller moduli.

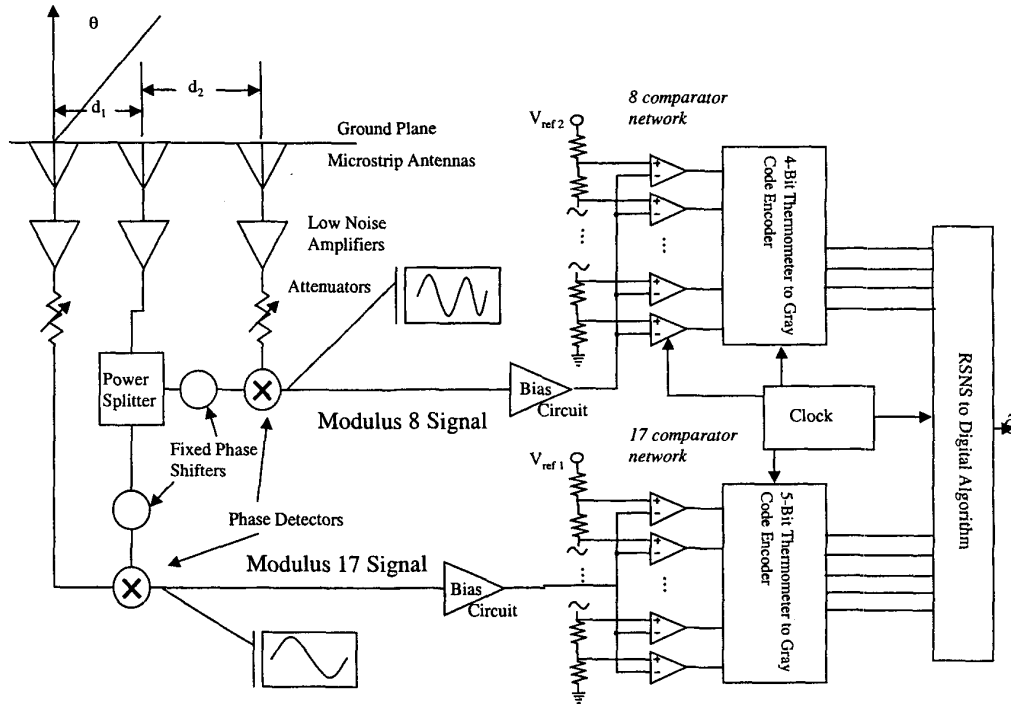
The dynamic range determines the angular resolution of the system and the antenna element spacing. A RSNS array based on  $N$  moduli ( $m_1, m_2, \dots, m_N$ ) has  $N + 1$  array elements. For an array using mixers for phase detection, the spacing between the reference element and element  $i$  is

$$d_i = \frac{\hat{M}\lambda}{4Nm_i}. \quad (3)$$

Table 1: Comparison of Dynamic Range of RSNS and OSNS.

System	Modulus	0	1	2	3	4	5	6	7	8	9	10	11	12	13	14	15	16	17	18	19	20	21
RSNS	$m_1=3$	0	0	1	1	2	2	3	3	2	2	1	1	0	0	1	1	2	2	3	3	2	2
	$m_2=4$	0	1	1	2	2	3	3	4	4	3	3	2	2	1	1	0	0	1	1	2	2	3
OSNS	$m_1=3$	0	1	2	2	1	0	0	1	2	2	1	0	0	1	2	2	1	0	0	1	2	2
	$m_2=4$	0	1	2	3	3	2	1	0	0	1	2	3	3	2	1	0	0	1	2	3	3	2

Figure 1: RSNS Direction Finding Antenna Architecture.



To demonstrate the RSNS antenna, a two channel system was selected with modulus of  $m_1=8$  and  $m_2=17$ . The prototype architecture is shown in Fig. 1. Three receiving elements are used to measure an 8 GHz incident signal. The receiving elements are microstrip dipoles designed for 8 GHz. The spacing between elements is defined by (3). A summary of the system parameters is shown in Table 2 along with

those of the OSNS design for comparison. Each channel contains a low noise amplifier and the center element serves as a common element for both interferometers. The phase detector output (PDO) for channel  $i$  is a symmetrical folding waveform

$$PDO_i(\theta) = \cos(kd_i \sin \theta + \phi_i) \quad (4)$$

where  $\phi_i$  is a known phase shift,  $k = 2\pi/\lambda$  and  $\theta$  is the angle of arrival. The separation between interferometer elements,  $d_1$  and  $d_2$ , defines the number of folding waveforms within the FOV

$$n_i = \frac{\hat{M}}{2m_i N} = \frac{2d_i}{\lambda} \quad (5)$$

System	OSNS	RSNS
Method	Experimental	Simulated
Moduli	6, 11	8, 17
Spacings (inches)	3.82, 2.08	1.18, 0.56
Resolution (ave)	2.02	2.08
RMS error (degrees, 120 degree FOV)	> 25	0.66
Dynamic range (bins)	66	64
Number of comparators	17	25
Frequency band (GHz)	8.2-10	7-8
Number of channels	2	2

Table 2: Prototype Antenna Comparison.



Figure 2: RSNS Folding Waveforms

A simulation of the detected phase (symmetrical folding waveform) is shown in Fig. 2. The  $m_1 = 8$  channel has two folds and the  $m_2 = 17$  channel has 0.941 folds as shown in the figure. The detected voltage is processed by a dc restoration amplifier to bring the folding waveform above dc so that the comparator threshold levels lie between ground and the bias voltage. The amplifier output is sampled in both channels by a small network of comparators. The normalized value for the 17 threshold levels is  $T = \cos(2n - 1/2m_i)$  for  $n=1$  to 17. A similar process can determine the threshold levels for the modulus 8 comparators. A channel with modulus  $m_i$  has  $m_i$  comparators (see Table 1). The number of comparators that are ON in each channel is mapped onto an EEPROM chip that converts the RSNS vector into a bin number that corresponds to a known AOA.

Using the phase waveforms shown in Fig. 2, the transfer function of the RSNS antenna is shown in Fig. 3. As is typical with phase scanned arrays, the  $\sin(\theta)$  dependence in (4) causes the folding waveforms to expand as the AOA diverges from broadside. Since the outputs from both channels expand at the same rate, the unique relative relationship between channels is maintained. However, it does increase the bin size resulting in reduced DF resolution for angles near endfire relative to those near broadside, as shown in Fig. 3.

The dynamic range for the prototype system is 64. This dynamic range was chosen to provide a 5-bit output for the angle of arrival. At broadside the bin width is  $1.6^\circ$  and at  $60^\circ$  off broadside, the bin width is  $3.4^\circ$ . More importantly, the RMS reporting error is  $0.66^\circ$  for the FOV of  $\pm 60^\circ$  off broadside and  $2.20^\circ$  over a  $180^\circ$  FOV.

The most significant impact of the Gray Code characteristic of the RSNS is the absence of encoding errors. Fig. 4 shows the experimental results from the OSNS DF antenna [3]. The OSNS does not possess Gray Code properties since multiple comparators are required to change state simultaneously at each code transition, resulting in large errors. The RSNS has the Gray Code property, so only one comparator must change state to transition between bins. If a comparator fails to change state at the correct AOA, the system will report that the signal is in the adjacent bin resulting in a small error.

### III. Conclusion

The robust symmetric number system provides a unique and innovative means of mapping directions of arrival in the spatial domain to a digital representation with no encoding errors. There are no theoretical limits on the array baseline or unambiguous AOA resolution. In the absence of noise and system errors, the minimum element spacing and AOA resolution are limited only by the physical size of the array elements and the complexity of the decoding electronics (i.e., number of comparators required).

The RSNS antennas have the potential to perform high resolution DF with very small baselines. The simplicity of the microwave components allows operation over wide bandwidths. The prototype antenna will be capable of a RMS DF error of less than one degree. The system's small weight and size make it an ideal candidate for small unmanned air vehicles.

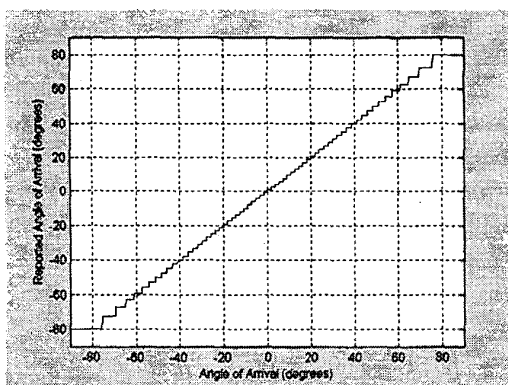


Figure 3: RSNS Transfer Function.

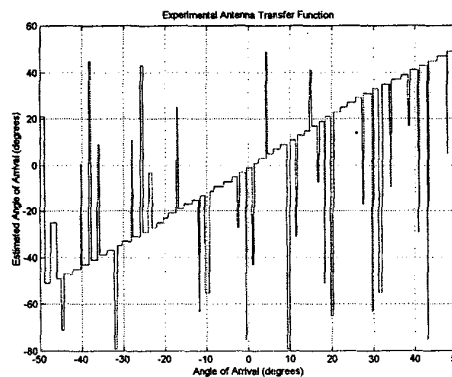


Figure 4: OSNS Transfer Function [3].

### IV. References

1. S. Lipsky, *Microwave Passive Direction Finding*, Wiley, 1987.
2. P. Pace, D. Styer, and I. Akin, "A Folding ADC Employing a Robust Symmetrical Number System with Gray Code Properties," ISCAS'98.
3. D. Jenn, P. Pace, T. Hatzithanasiou, "High resolution wideband direction finding arrays based on optimum symmetrical number system encoding," *Electronics Letters*, Vol 34, No. 11, May 28, 1998, pp. 1062-1063.